Datasheet of Environment Board

1. Overview

The environmental sensing platform is an ESP32-S3–based embedded system designed for real-time acquisition of multi-modal environmental data.

It integrates a BME680 sensor for temperature, humidity, barometric pressure, and gas-based air-quality estimation, complemented by GPS-based spatiotemporal metadata and a VL53L4CX time-of-flight sensor for distance measurement. Sensor data are locally visualized on an OLED display, logged to removable storage, and transmitted over Wi-Fi via HTTP, WebSocket, and TCP interfaces. The modular I2C and SPI architecture enables straightforward expansion with additional sensors and peripherals for future applications.

2. Feature

ESP32-S3 microcontroller with integrated Wi-Fi connectivity for embedded and IoT applications:

- Atmospheric sensing via BME680:
  - Temperature
  - Relative humidity
  - Barometric pressure
  - Gas resistance–based air quality (IAQ)
- Global Navigation Satellite System (GNSS):
  - Position (latitude, longitude)
  - Time and date synchronization
- 128x64 OLED display (SSD1306) for real-time visualization of system status and sensor readings
- MicroSD card support for continuous data logging and offline analysis
- TOF sensor used to measure height
- Wireless networking interfaces:
  - Embedded HTTP server with dashboard
  - WebSocket interface for real-time data streaming
  - TCP server for command-line data retrieval
- Peripheral expansion interfaces:
  - I2C bus for additional digital sensors
  - SPI bus for high-speed peripherals e.g. SD card

3. PCB Design and Consideration

3.1 Objectives & Schematics

This PCB is used to integrate an environmental sensor system onto a single board, achieving a reliable connection to the modules, making it easy to install into a 3D printed casing and perform indoor/outdoor measurements. The system is mainly controlled and processed by ESP32-S3 Feather, with external devices including BME environmental sensors, ToF distance sensors, GPS modules, OLED display screens, and MicroSD.
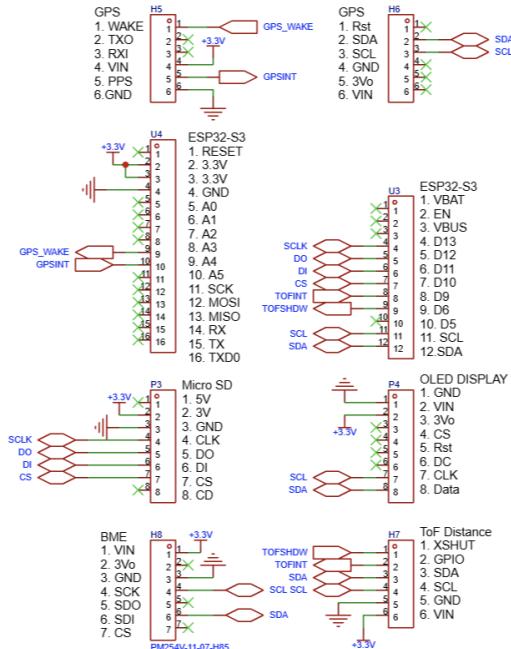
Figure 1 Schematic of Environment Sensor
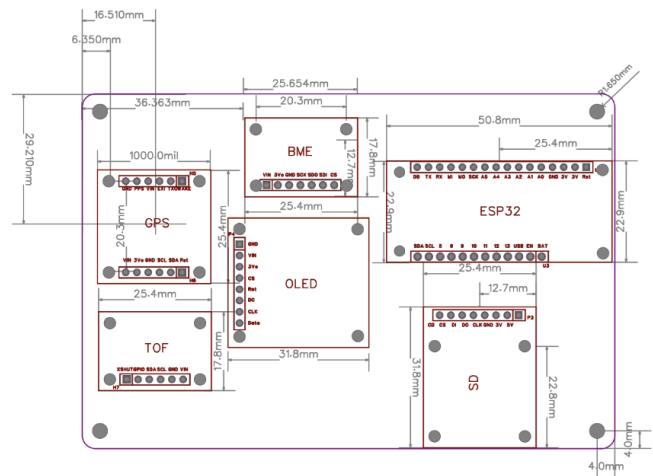
Figure 2 Board and mounting hole dimensions (in mm)

3.2 Circuit Routing & Signal Integrity & Layout

The BME, ToF, and GPS modules share the same I²C bus (SDA/SCL), using a short, straight, and less via wiring strategy to avoid excessive bus capacitance and waveform distortion caused by long stubs, while reducing the risk of crosstalk. High-current peripherals such as the OLED and SD card were placed relatively close to the ESP32-S3 to minimize voltage drop and transient supply disturbance. MicroSD and OLED adopt SPI to meet write

throughput requirements, reduce display latency, and improve interactive experience.

The PCB outline, mounting hole positions, and module placement were chosen to align with the enclosure geometry, ensure unobstructed optical paths for the ToF sensor, and provide sufficient clearance from board edges to maintain mechanical robustness and manufacturability.
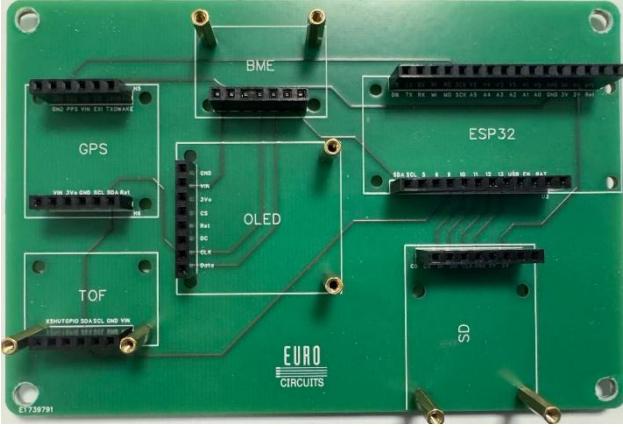

Figure 3 PCB Structure

3.3 Power Management

The entire system is powered by a 45W portable power bank. The portable power bank supplies power to the ESP32-S3 Feather through its Type-C input. The onboard power management and regulation circuit of Feather subsequently generates the required 3.3V voltage rail, which is used as the main logic and sensor power supply domain. All peripherals share a common 3.3 V and GND reference voltage to ensure consistent compatibility with ESP32-S3. This method simplifies system integration, avoids the use of multiple external voltage regulators, and enables reliable portable operation of indoor/outdoor environment perception demonstrations.

4. 3D Enclosure Design and Print

4.1 Functionality

The enclosure was designed to protect and organize an Environmental Board comprising a ToF distance sensor, LED/OLED display, BME environmental sensor, GPS module, and microSD logging, while allowing each sensing element to operate without obstruction. A two-layer base was adopted: the upper level secures the PCB, and the lower cavity holds a power bank, which improves robustness by separating electronics. Dedicated apertures were introduced for each interface: a central window for the display, ventilation openings for the BME to exchange air with the ambient environment (enabling temperature/IAQ measurements rather than internal board

temperature) and aligned openings for GPS and ToF to ensure unobstructed signal reception and ranging.
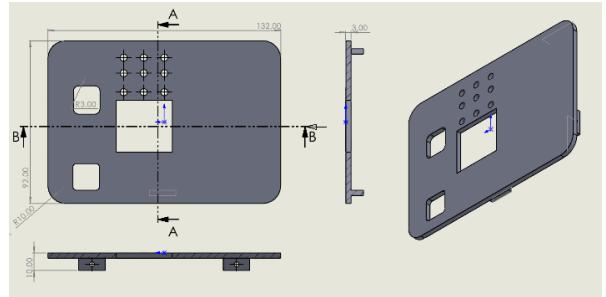

Figure 4 3D Model of Enclourse Design(TOP)
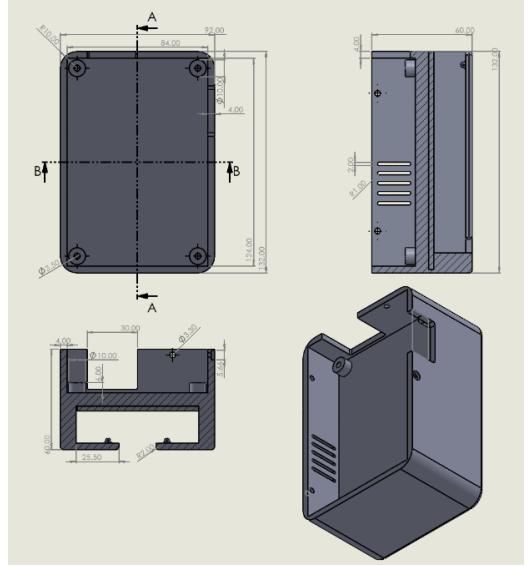
Figure 5 3D Model of Enclourse Design(Bottom)

4.2 Fit and assembly

The PCB is constrained by internal ledges/standoffs and fixed using screw bosses to prevent movement during handling. Clearance around the PCB outline and component height was intentionally included to avoid mechanical interference when the lid is installed, and the power bank cavity was sized with insertion/removal allowance for repeatable fitting. The enclosure uses a lid–base screw connection for reliable closure and straightforward maintenance, allowing fast access to the PCB, SD card, and wiring during testing.

4.3 Aesthetics

A rounded-rectangle profile and consistent radius were used to produce a clean and compact appearance. Openings were grouped by function (display, ventilation, and sensor windows) to keep the external geometry visually ordered while maintaining sensor performance.

4.4 Printability

The enclosure geometry was designed to be 3D-print

friendly, with minimal support required. The base can be printed open side up to avoid support inside the cavities, while the lid can be printed flat to preserve hole accuracy. Wall thickness, fillets, and reinforced screw bosses improve strength and reduce the risk of cracking, and small clearances were included to account for typical 3D printing tolerances.

4.5 Design rationale and iterations

Several iterations were required, particularly for the lid, because early versions lacked sufficient and well-positioned openings. In initial prototypes, the GPS aperture was too small or misaligned, leading to poor satellite reception. Limited exposure of the ToF window and inadequate BME ventilation also caused unreliable ranging and environmental readings. The final design increased and repositioned the GPS and ToF apertures, and expanded BME ventilation (perforations and side slots) to improve airflow and heat dissipation.

5. Data Acquisition and Data Pipeline
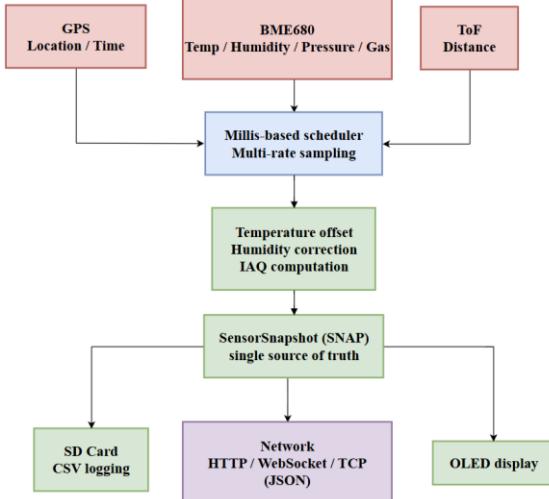
Figure 6 Data Pipeline

5.1 Firmware Architecture and Data Workflow

The data acquisition procedure is implemented in an ESP32-S3 microcontroller. All data from sensors are written into a unified structure SensorSnapshot (SNAP), which is the only output of the whole system to CSV storage, WebSocket transmission as well as local display. This ensures consistent and time-aligned output.

5.2 Interface and Connectivity

All sensors and the OLED display share a single I²C bus configured at 400 kHz (SDA=GPIO3, SCL=GPIO4). The SD card is accessed via an SPI bus (SCK=GPIO13,

MISO=GPIO12, MOSI=GPIO11, CS=GPIO10). We also implement multiple data access methods to support demonstrations and offline analysis:

HTTP (Port 80): GET /API/sensors returns the latest JSON snapshot; GET / provides a lightweight dashboard; GET /health returns an active response $'OK'$.

WebSocket (Port 81): Pushes a stream of JSON snapshots to connected browsers/clients; sends the latest snapshot immediately upon client connection.

TCP stream (port 5000): Console-style access supporting simple commands ($help, json, id, oled < text >$) and periodic JSON output, suitable for scripting/debugging.

5.3 Sampling, Logging and Output Rates

Sampling and output are implemented using non-blocking, timer-triggered tasks, which are scheduled in milliseconds). Different sampling rates are employed to match sensor dynamic characteristics and reduce storage overhead.

Table 1 System Task Scheduling Configuration

Task / Source	Period	Rationale
Environmental sensing (BME680)	0.5 s	Slow-changing variables; adequate temporal resolution
GPS parsing	1 Hz	Maintain updated position/time when available
SD CSV logging	3 s	Reduce SD dataset size while preserving trends
WebSocket broadcast	5 s	Live dashboard updates without heavy network load
OLED refresh	1 s	Human-readable UI responsiveness
Serial debug output	2 s	Development and validation

5.4 Data Formatting

CSV is used to store data from Snapshot. The schema of CSV is shown below: timestamp, time, date, temp_C, humidity_pct, pressure_kPa, iaq, fix, lat, lon, sats.

When GPS date/time is valid, timestamp uses GPS-derived time ($YYYYMMDD - HHMMSS$). Otherwise, the system falls back to a boot-based timestamp ($boot + Xs$) to preserve monotonic ordering and continuous logging. The fixed flag (1/0) and sensor validity flags are used to identify invalid or missing

measurements.

5.5 On-device calibration and derived metrics

Basic calibration and a derived air-quality indicator are computed on-device before logging and transmission to improve usability and to minimize systematic offsets.

Temperature offset correction:

$$T_{cal} = T_{raw} - 5\text{°C} \tag{1}$$

This compensates for a consistent positive temperature bias observed during our data collection activity in Vauxhall Station and Battersea Power Station.

Humidity correction after temperature calibration (Magnus-based scaling):

Saturation vapor pressure is approximated as:

$$e_s(T) = 6.112 \cdot e^{\frac{17.62T}{243.12+T}} \tag{2}$$

Relative humidity is scaled to remain consistent after temperature correction:

$$RH_{Cal} = RH_{raw} \cdot \frac{e_s(T_{raw})}{e_s(T_{cal})} \tag{3}$$

Finally, RH_{Cal} is clipped to the physically valid range [0,100] %.

IAQ-like scalar from gas resistance:

An indicative IAQ-like index is computed from BME680 gas resistance RRR using a baseline R0:

$$IAQ = 100 \cdot \left(\frac{R_0}{R}\right)^{1.4} \tag{4}$$

The index is bound to [0,500] to prevent outliers dominating visualization and to provide a stable qualitative indicator for scenario comparison.

5.6 Robustness features for long-duration runs

Wi-Fi reconnection: the device periodically retrieves Wi-Fi association if disconnected, while continuing sensing and SD logging.

Validity flags: sensor availability is tracked (bme_ok) and exported, allowing downstream analysis to filter invalid samples rather than silently using stale values. Single snapshot state (SNAP): prevents inconsistencies between what is displayed, logged, and transmitted, improving reproducibility during demonstrations and experiments.

6. Data Collection and Comparison

6.1 Overview of Collected Data

Two-day environmental data collection (December 6–7) at multiple outdoor locations across London, including public parks, residential areas, traffic-exposed roads. Each site captured measurements of temperature, relative humidity, atmospheric pressure, and an air quality indicator (AQI), and compared with publicly available reference data in Table 2.

Table 2 Environmental Sensor Parameter comparison [1-3]

Site	Time	Variable	Tested	Ref
St. James Park	10	Temp.	11.5	11.2
		Humi.	70.04	69
		Press.	99.74	--
	11	Temp.	11.8	12.8
		Humi.	63.39	62
	10/11	AQI	45	36
Old Kent Rd.	15	Temp.	14.1	14.6
		Humi.	88.21	87
		Press.	98.86	--
	16	Temp.	14.8	14.6
		Humi.	83.33	85
	15/16	AQI	51	36
Northolt	21	Temp.	12.2	12.0
		Humi.	80.35	73.8
		Press.	98.41	99.9
Wimbledon	10:10	Temp.	11.3	11.5
		Humi.	83.43	86
		Press.	100.83	100.03
		AQI	47	54
Hammersmith	12:30	Temp.	12.5	12.7
		Humi.	82.33	88
		Press.	99.35	--
		AQI	37	47

Multi-site approach enables the evaluation of sensor performance under varying environmental exposure conditions, holding direct relevance for standardizing and expanding public health monitoring.

6.2 Temperature Comparison

In all monitoring stations, measured temperatures align well with reference data, typically within ±1°C.

At St James's Park, the 10:00 temperature reading (11.5 °C) closely matched the benchmark (11.2 °C), while the 11:00 measurement (11.8 °C) showed a larger deviation from the reference (12.8 °C). Near Old Kent Road, deviations at both time points remained below 0.5 °C, indicating stable sensor performance even in traffic-influenced environments. Similar consistency was observed in Wimbledon and Hammersmith, where measured values differed from reference data by less than 0.3–0.5 °C. Overall, these results demonstrate that the

temperature sensors provide reliable data for slowly varying environmental conditions and are suitable for environmental monitoring and public health surveillance.

6.3 Relative Humidity Comparison

Relative humidity measures exhibit greater deviation compared to temperature, particularly in urban areas.

At St. James's Park, measured humidity values (70.04% and 63.39%) were close to benchmark values (69% and 62%), indicating good agreement in open green spaces. Near Old Kent Road and in the Hammersmith area, observed values were up to 5-6% lower than benchmarks, showing significant differences. The humidity measured at Northolt (80.35%) exceeded the benchmark (73.8%), suggesting potential influence from local microclimate effects.

Such deviations fall within expected ranges, as humidity is highly sensitive to local airflow, surface moisture, and sensor placement, while benchmark data typically represent regional averages. Nevertheless, the measured values remain within reasonable limits and maintain the overall environmental trend.

6.4 Atmospheric Pressure Comparison

The measured atmospheric pressure values align closely with existing reference data. At the Northolt site, the measured pressure (98.41 kPa) is extremely close to the reference value (99.9 kPa). Deviations at Wimbledon site remained below 1 kPa: measured values were 100.83 kPa and 101.20 kPa, compared to reference values of 100.03 kPa and 100.07 kPa.

Given the relative stability of atmospheric pressure over short time scales, such precise agreement indicates well-calibrated sensors and a stable system, providing reliable assurance for the overall data acquisition process.

6.5 Air Quality Index (AQI Class) Comparison

Compared to baseline data, AQI Class values exhibit the most pronounced variation in traffic-dense areas. At St. James's Park, the measured AQI Class value (45) exceeded the baseline (36), indicating moderately elevated local exposure levels. Near Old Kent Road, the observed AQI Class value (51) surpassed the baseline (36), consistent with pollution intensification driven by road traffic. Conversely, measured AQI Class values in Wimbledon and Hammersmith were below the baseline, reflecting potential spatial variability and short-term fluctuations.

Furthermore, this system calculates qualitative indoor air quality indices based on local gas resistance measurements, while reference AQI values originate from regional monitoring networks. This discrepancy highlights the system's capability to capture localized air quality variations—subtle fluctuations, often not reflected in regional average datasets.

6.6 Overall Performance Evaluation and Consideration

Overall, the environmental sensing system demonstrated excellent performance for slowly varying parameters, particularly temperature and atmospheric pressure—with measurements highly consistent with reference datasets across multiple locations and time points. This indicates that the sensing hardware, calibration strategy, and data acquisition process possess sufficient stability to meet environmental monitoring requirements.

Notably, the system provides real-time localized environmental information, which holds significant value for public health applications focused on individual exposure rather than regional averages. These results highlight the complementary role of low-cost portable sensing systems in augmenting existing environmental monitoring infrastructure.

For relative humidity and air quality indicators, deviations between local and overall environmental conditions resulted in less precise measurements. However, our system's ability to capture locally specific responses often holds greater practical value in public health assessments than absolute accuracy. From a public health perspective, individuals are exposed to street-level and pedestrian-level environments, not regional averages. Thus, by delivering granular real-time environmental data, this system enhances personal risk awareness while supporting urban planning decisions and community health research, thereby improving existing monitoring frameworks.

Reference:

[1] Met Éireann, "Weather Observations Website," Met Éireann. [Online]. Available: https://wow.met.ie/stations.

[2] Met Office, "Weather Observations Website (WOW)," Met Office. [Online]. Available: https://wow.metoffice.gov.uk/observations/details.

[3] IQAir, "Air Quality Data Platform," IQAir. [Online]. Available: https://www.iqair.com/gb/uk/england.

GitHub Link:

https://github.com/joywithmeldoy/Environment_Sensor_Group-7.git